



Electrospun ZnO Nanofiber Membranes for Photocatalytic Water Treatment: A Comparative Review of Fabrication Strategies

Aditya Rianjanu^{1,*}, Eka Nurfani¹, Tarmizi Taher²

¹Department of Materials Engineering, Faculty of Industrial Technology, Institut Teknologi Sumatera, Lampung, Indonesia

²Department of Environmental Engineering, Faculty of Infrastructure and Regional Technology, Institut Teknologi Sumatera, Lampung, Indonesia

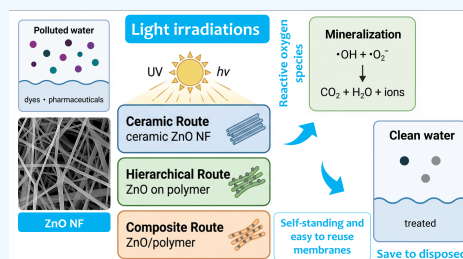
✉ Corresponding author: aditya.rianjanu@mt.itera.ac.id

ARTICLE HISTORY: Received: April 10, 2026 | Revised: May 2, 2026 | Accepted: May 5, 2026

ABSTRACT

Electrospun ZnO nanofiber membranes are promising candidates for photocatalytic water treatment, offering directional charge transport, high surface-to-volume ratio, and self-standing membrane architectures that enable straightforward catalyst retrieval and reuse, a critical advantage over dispersed semiconductor nanoparticle systems where post-treatment recovery remains a major bottleneck. However, the fabrication route fundamentally determines membrane morphology, mechanical integrity, retrievability, and photocatalytic performance. This review classifies electrospinning-based fabrication into three routes: the Ceramic Membrane Route (precursor/polymer blending followed by calcination), the Hierarchical Membrane Route (secondary ZnO growth on electrospun polymer scaffolds), and the Composite Membrane Route (direct electrospinning of pre-synthesized ZnO/polymer dispersions). The Ceramic Membrane Route yields high-crystallinity membranes with up to 100% pollutant degradation but poor mechanical integrity that hinders membrane retrieval. The Composite Membrane Route provides single-step fabrication with the best demonstrated reusability (10 cycles at 97–99% retention), 200-fold lower zinc leaching, and excellent mechanical robustness for repeated retrieval and deployment, positioning it as one of the more operationally mature options for near-term deployment. The Hierarchical Membrane Route delivers the highest surface area, the fastest degradation kinetics, and uniquely combines photocatalysis with membrane filtration in a single device, making it a particularly promising long-term direction once its multi-step processing is streamlined and continuous-flow scale-up is realized. This comparative framework guides the selection of fabrication strategy based on membrane retrievability, performance, and development-stage requirements.

Keywords: ZnO nanofiber membrane; electrospinning; photocatalytic membrane; water treatment; catalyst recovery; membrane reusability



1. INTRODUCTION

Water pollution by synthetic organic compounds (including industrial dyes, pharmaceuticals, and endocrine-disrupting chemicals) poses a severe threat to aquatic ecosystems and human health worldwide. Conventional wastewater treatment methods such as adsorption, coagulation, and biological processes often fail to completely mineralize recalcitrant organic pollutants, necessitating the development of advanced oxidation processes (AOPs). Among AOPs, semiconductor photocatalysis has emerged as a particularly promising approach because it can harness solar energy to generate highly reactive oxygen species (ROS) capable of degrading a wide range of organic contaminants into harmless products under ambient conditions [1,2].

Zinc oxide (ZnO) is one of the most extensively studied photocatalysts owing to its favorable properties: a direct wide band gap of 3.37 eV, high exciton binding energy of 60 meV, non-toxicity, abundance, low cost, and versatile morphology control. ZnO exhibits photocatalytic activity comparable to or exceeding that of TiO₂ for certain organic pollutants, and its hexagonal wurtzite crystal structure supports diverse nanostructured forms. However, practical application of ZnO in photocatalysis is constrained by several intrinsic limitations: rapid recombination of photogenerated electron–hole pairs,

activation only under ultraviolet (UV) light (which constitutes merely 4–5% of the solar spectrum), and susceptibility to photocorrosion in aqueous environments [3,4].

The morphology of photocatalytic materials profoundly influences their performance. One-dimensional (1D) nanofiber structures offer distinct advantages over nanoparticulate forms: (i) directional charge transport along the fiber axis that reduces recombination pathways, (ii) high surface-to-volume ratios that increase the density of catalytically active sites, (iii) interconnected fibrous networks that form self-standing membranes enabling facile catalyst recovery and reuse, and (iv) tunable porosity for enhanced mass transport of reactants and products. Critically, the membrane form factor addresses one of the most persistent practical challenges in semiconductor photocatalysis: catalyst retrieval. Dispersed nanoparticle photocatalysts require energy-intensive post-treatment separation (centrifugation, filtration, or magnetic recovery) [4,1], whereas self-standing nanofiber membranes can be simply lifted from the treated water and redeployed, dramatically simplifying operational workflows and reducing secondary waste [5,6]. These attributes make nanofibers particularly attractive for membrane-integrated photocatalytic water treatment systems.

Electrospinning has established itself as the primary tech-

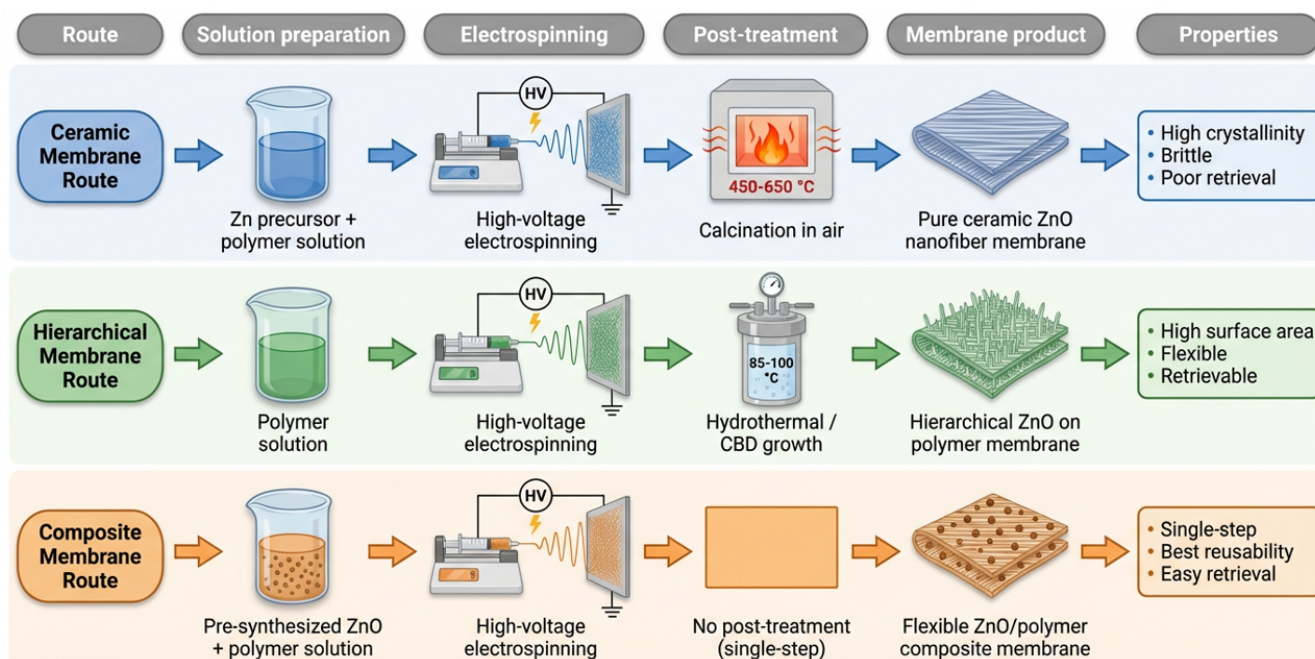


Figure 1. Schematic illustration of the three electrospinning-based fabrication routes for ZnO nanofiber photocatalytic membranes, showing the process steps and resulting membrane products. The Ceramic Membrane Route requires high-temperature calcination yielding brittle membranes; the Hierarchical Membrane Route involves secondary ZnO growth on polymer scaffolds; and the Composite Membrane Route offers single-step fabrication of flexible, easily retrievable membranes.

nique for producing 1D nanofibers with controlled morphology and composition. This versatile method employs a high-voltage electrostatic field to draw a polymer solution or melt into ultrafine fibers with diameters ranging from tens of nanometers to several micrometers. The technique is simple, cost-effective, and scalable from laboratory single-needle setups to industrial needleless or multi-jet configurations [7,8]. Crucially, electrospinning offers multiple pathways for incorporating ZnO into nanofiber structures, and these different fabrication routes produce fundamentally different products, from pure ceramic nanofibers to flexible polymer/ZnO composite membranes.

Several recent reviews have addressed adjacent aspects of this field. Nasir et al. [9] surveyed electrospun nanofibrous photocatalytic membranes for wastewater treatment, focusing predominantly on TiO₂-based systems. Cordoba et al. [10] provided a brief review of polymer/semiconductor hybrid nanofibers as photocatalysts for water remediation. Mapukata et al. [11] reviewed the fabrication, modification, and application of both TiO₂ and ZnO electrospun nanofibers for organic pollutant degradation, but treated the two oxides in parallel without distinguishing between fabrication routes for ZnO. Serik et al. [12] examined photocatalytic applications of electrospun nanofibers across multiple semiconductor materials, while Mhalshekar et al. [13] surveyed sustainable wastewater remediation strategies using electrospun nanofiber photocatalysts in general. Adjacent reviews on electrospun nanofibers for organic dye photocatalysis [14], photocatalytic water splitting and hydrogen generation [15], and electrospun semiconductor heterostructure nanofibers for photocatalytic energy conversion and remediation [16] are likewise organized by mechanism, heterostructure type, or application target rather than by the electrospinning-route taxonomy that determines membrane

retrievability. ZnO-specific reviews have largely focused on modification strategies such as doping, heterojunction formation, and cocatalyst loading [17,3], on specific application domains [4,18], on ceramic nanofiber preparation broadly [19], or on electrospun nanofiber membranes for dye filtration [20]. More recent ZnO-photocatalysis reviews have systematically surveyed visible-light activation [21,22,23], metal/non-metal doping and heterojunction engineering [24,25,26,27,28], broad synthesis-method comparisons of ZnO nanostructures [29,30,31,32], dual ZnO/TiO₂ synthesis-and-modification frameworks [33,34], and ZnO photocatalysis surveys for specific application classes [35,36], but they do not adopt an electrospinning-route lens for membrane-format ZnO photocatalysts. A complementary body of work has analyzed the photoreactor and catalyst-recovery challenges that motivate membrane-immobilized photocatalyst formats [37], reinforcing the importance of the fabrication-route-driven retrievability framework adopted here.

We acknowledge that several of the reviews cited above touch upon ZnO/electrospinning fabrication strategies, in some cases at length. The contribution of the present review is therefore not the mere existence of fabrication-related discussion in the literature, but rather a *specific reframing* of that literature. In particular, no prior review has, to the best of our knowledge, systematically examined how the choice of electrospinning-based fabrication route itself determines the morphology, crystallinity, mechanical integrity, retrievability, and ultimately the photocatalytic performance of ZnO nanofiber *membranes* (rather than nanofiber powders or coatings). The present review addresses this gap by adopting a *fabrication-route-centric* perspective: the same ZnO composition processed through different electrospinning routes yields products with dramatically different characteristics, including brittle ceramic mats versus flexible

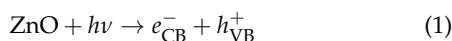
composite membranes, surface-exposed crystallites versus polymer-embedded particles, and stationary batch reactors versus retrievable continuous-flow membranes. Distinguishing this work from prior reviews, we (i) restrict the scope to ZnO (rather than treating it alongside TiO₂); (ii) classify the literature into three discrete fabrication routes with distinct process steps and product forms; (iii) place explicit emphasis on membrane retrievability and reusability as practical figures of merit for semiconductor photocatalysts; and (iv) provide a head-to-head comparison framework that directly informs route selection for membrane-based water treatment applications.

This review addresses this gap by classifying electrospinning-based ZnO nanofiber membrane fabrication into three distinct routes (Fig. 1). The **Ceramic Membrane Route** combines precursor/polymer blending with electrospinning and calcination, yielding pure ceramic ZnO nanofiber membranes. The **Hierarchical Membrane Route** couples electrospinning of polymer scaffolds with secondary ZnO growth (hydrothermal, chemical bath deposition, etc.), creating hierarchical ZnO/polymer membrane structures. The **Composite Membrane Route** disperses pre-synthesized ZnO nanoparticles into polymer solutions before electrospinning, forming flexible ZnO/polymer composite membranes. For each route, the fabrication parameters, resulting morphologies, membrane characteristics, retrievability, and photocatalytic performance are systematically analyzed and compared based on literature published between 2013 and 2026. This comparative framework aims to guide researchers in selecting the most appropriate fabrication strategy based on target membrane application requirements, with particular attention to the ease of catalyst retrieval and reuse that each route affords.

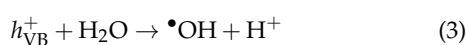
2. FUNDAMENTALS

2.1 Photocatalysis mechanism on ZnO

ZnO crystallizes predominantly in the hexagonal wurtzite structure (space group $P6_3mc$), characterized by a direct band gap of approximately 3.37 eV at room temperature [38,39]. Upon irradiation with photons of energy equal to or exceeding the band gap energy (typically UV light with $\lambda \leq 368$ nm), electrons in the valence band (VB) are excited to the conduction band (CB), generating electron-hole (e^-/h^+) pairs as described by Eq. 1:



The photogenerated charge carriers migrate to the ZnO surface, where they participate in redox reactions with adsorbed species (Fig. 2). Conduction band electrons reduce dissolved molecular oxygen to form superoxide radical anions ($\bullet\text{O}_2^-$; Eq. 2), while valence band holes oxidize water or surface hydroxyl groups to produce hydroxyl radicals ($\bullet\text{OH}$; Eq. 3):



These ROS ($\bullet\text{OH}$, $\bullet\text{O}_2^-$, and h^+ themselves) are powerful oxidants that can non-selectively degrade organic pollutants through successive oxidation steps, ultimately achieving mineralization to CO₂, H₂O, and inorganic ions. Scavenger studies across the reviewed literature consistently identify

h^+ as the dominant active species for ZnO nanofiber systems [40,41], followed by $\bullet\text{O}_2^-$ [42,43] and $\bullet\text{OH}$ [44].

The photocatalytic efficiency of ZnO is limited by three primary factors: (i) fast bulk recombination of e^-/h^+ pairs (occurring within nanoseconds), which dissipates the absorbed photon energy as heat; (ii) restriction to UV light activation, which limits solar energy utilization; and (iii) photocorrosion in aqueous media, where photogenerated holes oxidize the ZnO lattice itself ($\text{ZnO} + 2h^+ \rightarrow +\frac{1}{2}\text{O}_2$), gradually dissolving the catalyst [45]. Strategies to address these limitations, including nanostructure engineering, heterojunction formation, and doping, are inherently linked to the fabrication route employed, as discussed in subsequent sections.

2.2 Electrospinning basics

Electrospinning generates continuous nanofibers by applying a high-voltage electric field (typically 10–30 kV) to a polymer solution dispensed through a spinneret [7,46]. When the electrostatic force overcomes surface tension, a charged jet emerges from the Taylor cone formed at the needle tip. The jet undergoes bending instabilities and whipping motions that stretch and thin the fiber while the solvent evaporates, depositing dry nanofibers on a grounded collector [8,47].

The morphology and diameter of electrospun fibers are governed by solution parameters (polymer concentration, molecular weight, viscosity, conductivity, and surface tension), process parameters (applied voltage, flow rate, and tip-to-collector distance), and ambient conditions (temperature and humidity). For example, increasing the PVA polymer concentration from 8 to 10 wt% can change the bulk electrical conductivity of the resulting nanofiber mat from 0.03 microsiemenspercm to 1.20 microsiemenspercm, illustrating how solution parameters propagate to functional properties of the final membrane [48]. Polymer blending strategies provide an additional handle: blending polysulfone (PSU) into a PAN spinning dope tunes the water contact angle of the resulting electrospun mat from 14 degree (hydrophilic) to over 156 degree (superhydrophobic) without altering the underlying electrospinning setup [49]. Such hydrophobicity tuning is particularly relevant for floating photocatalytic membranes intended to skim contaminated water surfaces.

A persistent practical limitation of as-spun nanofiber mats is their modest mechanical strength, which can compromise membrane retrieval and reuse. Post-electrospinning treatments such as solvent vapor exposure can dramatically improve the mechanical properties: DMF vapor treatment of electrospun PVA nanofibers has been shown to increase tensile strength by up to 115% via physical crosslinking at fiber junction points [50]. Multi-component fiber compositions are another route to mechanical and functional robustness; for instance, PAN/PSU/PTFE composite nanofibers fabricated by single-step electrospinning combine high mechanical integrity, superhydrophobicity, and thermal stability up to 300 celsius, demonstrating how a single spinning step can deliver membranes that withstand demanding operating environments [51].

For ZnO nanofiber fabrication, these solution and process parameters must be co-optimized with the inorganic component, whether it is a dissolved zinc salt precursor (Ceramic Membrane Route), absent during spinning but added post-fabrication (Hierarchical Membrane Route), or a pre-formed ZnO particulate dispersion (Composite Membrane Route). Setup variants relevant to ZnO nanofiber photocatalysts include single-needle electrospinning (the most common config-

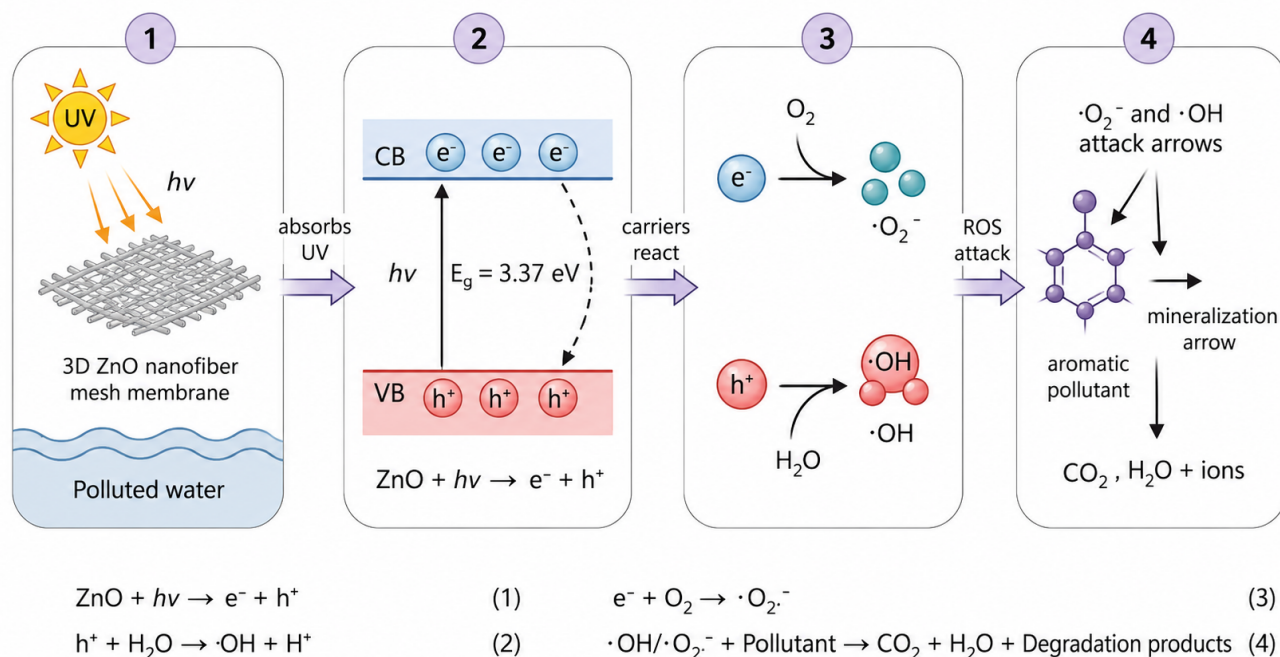


Figure 2. Photocatalytic mechanism on a ZnO nanofiber membrane: UV photon absorption generates electron–hole pairs across the 3.37 eV band gap; conduction band electrons reduce dissolved O₂ to superoxide radicals ($\cdot\text{O}_2^-$) and valence band holes oxidize H₂O to hydroxyl radicals ($\cdot\text{OH}$); these reactive oxygen species mineralize organic pollutants into CO₂, H₂O, and inorganic ions.

uration) and coaxial electrospinning for core–shell or hollow fiber architectures [52,53]. For comprehensive treatment of electrospinning fundamentals and recent developments in functional electrospun membranes, readers are referred to established reviews in the field [7,8,46].

3. CERAMIC MEMBRANE ROUTE

3.1 General process

The Ceramic Membrane Route is the most widely reported route for fabricating ZnO nanofiber photocatalysts. The process involves three sequential steps: (1) dissolving a zinc salt precursor and a carrier polymer in a compatible solvent system to form a homogeneous spinning solution, (2) electrospinning this solution into composite nanofibers containing the zinc precursor embedded within the polymer matrix, and (3) calcinating the as-spun fibers at elevated temperatures (typically 400–650 °C) in air to decompose the polymer template and crystallize ZnO. The product is a pure ceramic ZnO nanofiber membrane.

3.2 Precursor systems

The choice of zinc precursor, carrier polymer, and solvent system significantly influences the electrospinnability, fiber morphology, and final ZnO quality. Table 1 summarizes the precursor systems reported in the literature for the Ceramic Membrane Route.

Zinc acetate dihydrate ($\text{Zn}(\text{CH}_3\text{COO})_2 \cdot 2\text{H}_2\text{O}$) is overwhelmingly the most common precursor due to its high solubility in both aqueous and organic solvents and clean decomposition pathway. The most frequently employed carrier polymers are polyvinylpyrrolidone (PVP) dissolved

in DMF/ethanol mixtures [40,54,55], polyvinyl alcohol (PVA) in water [56,57], and polyacrylonitrile (PAN) in DMF [58,59]. Each polymer–solvent system offers distinct advantages: PVP/ethanol provides excellent electrospinnability and smooth fibers; PVA/water is environmentally benign; and PAN/DMF yields mechanically robust as-spun mats that maintain their shape during calcination. Notably, Flores-Garcia et al. [41] demonstrated the use of pork skin gelatin as a sustainable biopolymer template, where residual glycine chains acted as natural binding agents during calcination, eliminating the need for synthetic additives.

3.3 Effect of calcination

Calcination is the critical step that transforms the precursor/polymer composite into crystalline ZnO. The calcination temperature directly governs the crystallite size, surface area, and photocatalytic activity of the resulting nanofibers.

Singh et al. [58] systematically investigated calcination at 450, 550, and 650 °C for ZnAc/PAN nanofibers, observing that crystallite size increased from 29 to 41 nm while the fiber diameter decreased to approximately 60 nm at 650 °C. The resulting mesoporous nanofibers exhibited a BET surface area of 28.5 m²/g with a pore diameter of 2.39 nm. Most studies employ calcination temperatures in the range of 500–600 °C, which provides a balance between complete polymer removal, adequate ZnO crystallinity (confirmed by sharp XRD peaks corresponding to hexagonal wurtzite, JCPDS 36-1451), and retention of the fibrous morphology.

The heating rate also plays a crucial role: slow ramp rates (1–2 °C/min) help maintain the fiber structure by allowing gradual polymer decomposition, while rapid heating can cause fiber breakage. Chen et al. [40] used a controlled heat-

Table 1. Summary of photocatalytic and membrane performance for the Ceramic Membrane Route (precursor blending, electrospinning, and calcination).

Ref	Precursor System	Calcination	Fiber dia. (nm)	BET (m ² /g)	Target Pollutant	Light Source	Eff. (%)	Reusability
Singh [58]	ZnAc/PAN/DMF	450–650 °C, 1 h	~60	28.5	Naphthalene	UV 254 nm	100	6 cycles
Pantò [59]	ZnAc/PAN/DMF	600 °C, 2 h	~390	12.2	MB	UV 350 nm	96–99	NR
Chen [40]	ZnAc/PVP/DMF-EtOH	550 °C, 2 h	68±12	NR	RhB	UV 20 W	98	>85%, 3 cyc.
Flores-Garcia [41]	ZnAc/Gelatin/H ₂ O	550 °C, 3 h	<100	NR	MB	UV 253 nm	93.9	64%, 5 cyc.
Kim [54]	ZnAc/PVP/EtOH	600 °C, 5 h	237–279	NR	MB	UV 365 nm	99.2	NR
Meng [55]	ZnAc+CuAc/PVP	500 °C, 2 h	~115	61	Pyridine	Vis >420 nm	92.9	5 cycles
Liu [56]	ZnAc+Fe(NO ₃) ₃ /PVA	447 °C, 5 h	~77	NR	MB	UV Hg	–	NR
Naseri [57]	ZnAc/PVA/g-C ₃ N ₄	460 °C, N ₂	70±6	NR	MB	Sim. sun	91.8	NR

Table 2. Summary of photocatalytic and membrane performance for the Hierarchical Membrane Route (electrospun polymer scaffold with secondary ZnO growth).

Ref	Polymer Scaffold	ZnO Growth Method	ZnO Morphology	Target	Light	Eff. (%)	Reusability
Pan [42]	PVDF	Hydrothermal 95 °C, 3 h	Sm-ZnO nanowires	RhB	Sim. sun	99	5 cyc., stable
Araújo [62]	EDGT/TiO ₂	Hydrothermal 85 °C, 24 h	ZnO nanorods	RhB	Visible	90	NR
Yan [43]	PAN	Hydrothermal + PPy polym.	ZnO NRs + PPy	RhB	Sim. sun	97	79%, 5 cyc.
Chen [60]	PVDF	Hydrothermal 90–100 °C	ZnO nanorods	RhB	UV 254 nm	>powder	NR
Lu [44]	ZnO NFs	CuO hydroth. + Ag	CuO/Ag on ZnO	MB	Sim. sun	98.5	NR
Feng [63]	ZnO NFs	g-C ₃ N ₄ + Ag QDs	ZnO/g-C ₃ N ₄ /Ag	<i>E. coli</i>	Sim. sun	100 ^a	4 cyc., 100%

^aComplete bactericidal activity, not dye degradation.

ing rate of 2 °C/min to achieve well-preserved nanofibers with a diameter of 68 ± 12 nm. An unconventional approach was reported by Pantò et al. [59], who employed ice-bath quenching after calcination at 600 °C, which induced a hollow architecture with nanoplatelets (47 ± 6 nm diameter) and abundant grain boundary defects that enhanced photocatalytic activity.

The calcination atmosphere also influences the product: standard air calcination yields stoichiometric ZnO, while calcination under N₂ can generate carbonaceous residues from the polymer and introduce oxygen vacancies, as demonstrated by Naseri et al. [57] for ZnO/C/g-C₃N₄ nanofibers calcined at 460 °C under N₂ for only 15 min.

3.4 Morphology variants via the Ceramic Membrane Route

Beyond standard solid nanofibers, the Ceramic Membrane Route can produce several morphological variants through modification of the electrospinning configuration or post-treatment:

Solid nanofibers represent the standard product of single-needle electrospinning followed by calcination. Typical diameters range from 60 to 300 nm depending on the precursor loading and calcination conditions [58,40,54].

Hollow nanofibers are obtained through coaxial electrospinning with a sacrificial core. Cao and Xu [52] fabricated hollow ZnO nanofibers using PAN as the shell (containing zinc acetate) and PMMA as the sacrificial core, followed by selective removal of the core at 280 °C. The hollow structure was subsequently decorated with hydrothermally grown ZnO nanorods, achieving 94.7% MB degradation under UV light.

Porous nanofibers arise from phase separation during calcination or controlled defect introduction. The ice-bath quenching strategy of Pantò et al. [59] produced porous hollow fibers with enhanced photocatalytic activity attributed to abundant grain boundary defects and oxygen/zinc vacancies.

3.5 Photocatalytic performance of Ceramic Membrane Route products

Table 1 compiles the photocatalytic performance data for the Ceramic Membrane Route nanofibers. Pure ceramic ZnO nanofibers consistently demonstrate high photocatalytic activity under UV irradiation. The mesoporous ZnO nanofiber membranes reported by Singh et al. [58] achieved complete (100%) degradation of naphthalene within 12 min and anthracene within 14–68 min under 254 nm UV irradiation, with excellent reusability over 6 cycles. Kim et al. [54] reported 99.2% methylene blue (MB) degradation in 180 min under 365 nm UV light for pure ZnO nanofibers, which notably outperformed pure TiO₂ nanofibers prepared under identical conditions. Chen et al. [40] achieved 98% Rhodamine B (RhB) degradation in 2 h and additionally demonstrated antibacterial activity (96.22% against *E. coli* and 99.46% against *S. aureus*), with *h*⁺ identified as the dominant active species.

The incorporation of dopants or secondary phases via the Ceramic Membrane Route can extend the light absorption range and improve charge separation [17,19]. For instance, ZnO/CeO₂ composites exploit the Ce³⁺/Ce⁴⁺ redox couple to dynamically trap electrons and suppress recombination, achieving simultaneous degradation of mixed pharmaceutical and dye pollutants [18]. Fe-doping narrowed the ZnO band gap from 3.24 to 3.16 eV [56], while the p-CuO/n-ZnO heterojunction nanofibers of Meng et al. [55] achieved 92.9% pyridine degradation under visible light ($\lambda > 420$ nm) in 60 min with a rate constant of 0.0459 permin, demonstrating that the Ceramic Membrane Route is readily adaptable for visible-light-driven applications through compositional engineering.

A key limitation of Ceramic Membrane Route products is their mechanical brittleness after calcination, which makes handling difficult and severely compromises membrane retrieval and reuse; the calcined ceramic mat tends to fragment upon removal from treated water, limiting its use to batch reactor configurations where the membrane remains stationary.

4. HIERARCHICAL MEMBRANE ROUTE

4.1 General process

The Hierarchical Membrane Route employs a two-step (or multi-step) strategy: first, a polymer nanofiber scaffold is fabricated by electrospinning, and then ZnO nanostructures are grown directly on the fiber surfaces through a secondary process such as hydrothermal synthesis, chemical bath deposition (CBD), or sputtering. The polymer scaffold is typically retained in the final product, yielding a hierarchical structure that combines the flexibility of the polymer backbone with the photocatalytic functionality of the ZnO nanostructures. This route is distinguished from the Ceramic Membrane Route by the preservation of the polymer matrix and the formation of secondary ZnO architectures (nanorods, nanowires, nanoflowers) on the fiber surface rather than within the fiber bulk.

4.2 ZnO growth methods on electrospun scaffolds

Hydrothermal growth is the dominant method in the reviewed literature, employed in the majority of Hierarchical Membrane Route studies. The general protocol involves: (1) deposition of ZnO seed crystals on the polymer nanofibers, and (2) hydrothermal growth of ZnO nanostructures from an aqueous zinc salt/hexamethylenetetramine (HMTA) solution. Seed formation has been achieved through thermal decomposition of zinc acetate incorporated during electrospinning at relatively low temperatures (130–140 °C) [42,60,43], which is well below the decomposition temperature of most polymer scaffolds. The hydrothermal growth is typically conducted at 85–100 °C for 3–24 h in solutions of zinc nitrate hexahydrate or zinc chloride with HMTA, often with ammonia as a morphology-directing agent.

Chen et al. [60] conducted a comprehensive parametric study of hydrothermal growth on PVDF nanofiber templates, systematically varying temperature (50–140 °C), ammonia volume (0–7 mL), zinc-to-HMTA molar ratio (1:3 to 2:1), and growth time (1–5 h). They demonstrated that ZnO nanocrystals could form at only 140 °C on the nanofiber template, substantially lower than the >350 °C typically required for conventional ZnO crystallization, an effect attributed to the high surface reactivity at the nanoscale. Without pre-formed ZnO seeds, only disordered mixed nanorods/nanosheets were obtained, confirming the critical role of the seeding step for oriented nanorod growth.

Chemical bath deposition (CBD) was employed by Asghari Sarabi et al. [61] for growing ZnO nanorods on PAN nanofibers, followed by Ag nanoparticle deposition. This method enabled the creation of a floating nanofiber mat with combined photocatalytic, piezoelectric, and plasmonic functionalities.

4.3 Hierarchical structures and their characteristics

The most distinctive feature of the Hierarchical Membrane Route is the formation of hierarchical structures with significantly enhanced surface area compared to smooth nanofibers. Pan et al. [42] fabricated Sm-doped ZnO nanowires on PVDF nanofibers, achieving a biomimetic “Egeria-densalike” morphology that increased the BET surface area from 13.7 msquaredperg (undoped) to 17.5 msquaredperg (Sm-doped). The Sm doping simultaneously reduced the ZnO nanowire diameter and introduced oxygen vacancies, narrowing the band gap from 3.21 to 3.09 eV.

Araújo et al. [62] grew radially-oriented ZnO nanorods on TiO₂-decorated EDGT polymer fibers, creating a TiO₂/ZnO

hierarchical heterostructure where the BET surface area increased monotonically with hydrothermal growth time (optimal at 24 h). The photo-synergistic effect of the TiO₂/ZnO interface, confirmed by photoluminescence quenching, achieved 90% RhB degradation in 70 min under visible light.

Yan et al. [43] constructed a ternary ZnO/PPy/PAN system where ZnO nanorods (average length ~1647 nm) and polypyrrole (PPy) nanospheres were grown on PAN nanofibers via sequential hydrothermal and chemical oxidative polymerization steps. The n-p heterojunction between ZnO and PPy reduced the effective band gap from 3.22 to 2.65 eV, achieving 97% RhB degradation in 6 h under simulated sunlight with •O₂⁻ as the dominant active species.

4.4 Photocatalytic performance of Hierarchical Membrane Route products

Table 2 summarizes the photocatalytic performance data for the Hierarchical Membrane Route. The hierarchical structures produced by this route generally achieve the fastest degradation kinetics among the three routes. Lu et al. [44] reported the highest rate constant, with Ag/CuO/ZnO heterojunction nanofibers achieving 98.5% MB degradation in only 20 min under simulated sunlight (AM 1.5), corresponding to a rate constant 4.3–5.5 times higher than pure ZnO nanofibers. This exceptional performance was attributed to the triple-junction charge transfer pathway: the p-n CuO/ZnO interface facilitated charge separation while Ag nanoparticles served as electron sinks.

For antibacterial applications, Feng et al. [63] demonstrated 100% killing of both *E. coli* and *S. aureus* within 30 min under simulated solar light using Ag/ZnO/g-C₃N₄ nanofibers operating via a Z-scheme charge transfer mechanism. The system maintained complete bactericidal efficiency over 4 consecutive cycles.

A critical practical advantage of the Hierarchical Membrane Route is that the retained polymer scaffold provides mechanical flexibility and enables the formation of self-supporting, retrievable membranes that can be lifted intact from treated water for reuse. Pan et al. [42] demonstrated that their ZnO nanowire/PVDF membrane also functioned as a microfilter with a pore size below 0.08 μm and a water flux of 1620 Lpermsquaredperh, illustrating the dual photocatalytic-filtration functionality achievable through this route. The mechanical robustness of the polymer backbone ensures that the membrane can withstand repeated retrieval-redeployment cycles without structural degradation.

The primary limitations of the Hierarchical Membrane Route are the multi-step processing (which limits scalability), the batch nature of hydrothermal growth, and concerns about ZnO adhesion durability on the polymer surface during prolonged operation. Yan et al. [43] observed a decrease to 79% removal efficiency after 5 reuse cycles, which may partly reflect detachment of ZnO nanostructures from the fiber surface.

Table 3. Summary of photocatalytic and membrane performance for the Composite Membrane Route (direct electrospinning of pre-synthesized ZnO with polymer).

Ref	ZnO Type	Loading	Polymer Matrix	Target	Light	Eff. (%)	Reusability
Pascariu [67]	ZnO:La NPs	37 wt%	PVDF	MB	Visible	96.3	10 cyc., 97.6%
Yar [65]	ZnO NRs + TiO ₂	~20 wt%	PAN	MG	UV 254 nm	99	NR
Tissera [64]	ZnO NPs	11.5 wt%	PAN	MO	UV-A/B	~95	3 cyc., constant
Herath [68]	Cu-ZnO	40 wt%	CA	MB	Vis/sun	35	NR
Parangusan [66]	ZnO flowers	NR	PVDF	AZG, MG	Sunlight	85–90	NR
Pasindu [69]	GO-Ni-ZnO	5% Ni + 4% GO	CA	MB	Visible	93.4	NR
Jena [70]	CuO-ZnO	11–33%	PAN	CR	Sunlight	98	10 cyc., >99%

5. COMPOSITE MEMBRANE ROUTE

5.1 General process

The Composite Membrane Route is the most straightforward fabrication route: pre-synthesized ZnO nanostructures are dispersed into a polymer solution, and the mixture is directly electrospun into composite nanofiber membranes. No post-treatment (calcination or secondary growth) is required, making this a true single-step process for nanofiber membrane fabrication. The product is a flexible polymer membrane with ZnO particles either embedded within the fiber matrix or exposed on the fiber surface.

The ZnO component can take various pre-synthesized forms (nanoparticles [64], nanorods [65], nanoflowers [66], or doped/composite variants [67,68,69]), each prepared independently through established synthesis methods (sol-gel, hydrothermal, co-precipitation, or arc discharge) before incorporation into the electrospinning solution.

5.2 Key factors

5.2.1 Dispersion and loading optimization

The primary challenge in the Composite Membrane Route is achieving uniform dispersion of ZnO nanostructures within the polymer solution while maintaining electrospinnability. ZnO particles tend to agglomerate at high loadings, leading to beaded fibers, jet instability, or clogged needles. Ultrasonication is universally employed for dispersion, and the optimal loading typically falls in the range of 5–40 wt% depending on the particle size and polymer system.

Tissera et al. [64] incorporated 11.5 wt% ZnO nanoparticles (~35 nm) into PAN nanofibers (100–170 nm diameter), while Pascariu et al. [67] achieved loadings up to 37 wt% of lanthanide-doped ZnO in PVDF fibers with the aid of PVP as a sacrificial pore-forming component. Higher loadings generally increase photocatalytic activity but at the expense of fiber quality and mechanical properties.

5.2.2 ZnO exposure and accessibility

A critical limitation of the Composite Membrane Route is that ZnO particles partially embedded within the polymer matrix are not fully accessible for surface photocatalytic reactions. Tissera et al. [64] provided direct evidence of this through XRD analysis, showing that ZnO nanoparticles adopted a preferred crystallographic orientation inside the nanofibers with non-polar planes facing outward, which reduced photocatalytic activity compared to randomly oriented ZnO powder. This partial embedding explained why the degradation rate constant of PAN/ZnO nanofibers (0.317 perh) was 1.6 times lower than that of equivalent ZnO powder (0.533 perh).

To mitigate this limitation, Pascariu et al. [67] employed PVP as a sacrificial component that was removed by water washing to create pores exposing the embedded ZnO:Ln

nanostructures, achieving 96.33% MB degradation in 360 min under visible light with outstanding reusability (97.56% average efficiency over 10 cycles).

5.2.3 Polymer matrix selection

PVDF and cellulose acetate (CA) are the most commonly used polymer matrices in the Composite Membrane Route. PVDF offers chemical stability, hydrophobicity (contact angle up to 135 degree [66]), and piezoelectric properties that can synergistically enhance photocatalysis. CA provides biocompatibility, biodegradability, and has been successfully combined with Cu-ZnO [68] and GO-Ni-ZnO [69] for dual photocatalytic–antimicrobial applications. PAN is favored for its mechanical strength, solvent resistance, and the ability of its polar nitrile groups to adsorb cationic dyes, providing a synergistic adsorption–photocatalysis mechanism [65].

5.3 Photocatalytic performance of Composite Membrane Route products

Table 3 summarizes the photocatalytic data. The fastest degradation among Composite Membrane Route studies was reported by Pasindu et al. [69], who achieved 93.41% MB degradation in only 15 min under visible light using GO-Ni-ZnO/CA nanofibers, attributed to the triple synergy of Ni doping (band gap narrowing to 3.13 eV), GO (charge recombination suppression and enhanced surface area), and the high porosity of the electrospun membrane.

A distinguishing advantage of the Composite Membrane Route is the dramatically reduced zinc leaching compared to unsupported ZnO powder. Tissera et al. [64] quantified this using ICP-MS, finding that PAN/ZnO nanofibers leached only 40 ppb Zn (0.08%) versus 9067 ppb (18%) for free ZnO powder, a more than 200-fold reduction. This finding is critically important for practical water treatment applications where secondary contamination by dissolved zinc must be minimized.

The best reusability among all three routes was achieved by Composite Membrane Route materials, directly attributable to the excellent mechanical integrity that enables repeated membrane retrieval without structural damage. Pascariu et al. [67] demonstrated 10 consecutive retrieval-reuse cycles with 97.56% average efficiency for ZnO:La/PVDF membranes, and Jena et al. [70] achieved >99% efficiency retention over 10 cycles for calcined PAN/CuO-ZnO composites. This ease of retrieval eliminates the need for energy-intensive centrifugation or secondary filtration steps that are required when using dispersed semiconductor nanoparticle photocatalysts.

Several Composite Membrane Route studies demonstrated dual-function applications beyond photocatalysis: Parangusan et al. [66] combined photocatalytic dye degradation with oil absorption (115% oil uptake) using hydrophobic

PVDF/ZnO fibers, while Herath et al. [68] and Pasindu et al. [69] demonstrated combined photocatalytic and broad-spectrum antimicrobial activity with inhibition zones of 17–33 mm against both Gram-positive and Gram-negative bacteria.

6. COMPARATIVE ANALYSIS OF THE THREE ROUTES

6.1 Head-to-head comparison

Table 4 presents a systematic comparison of the three electrospinning-based fabrication routes across key performance and practical metrics. Each route occupies a distinct position in the trade-off space between photocatalytic performance, mechanical properties, and processing complexity.

A note on the comparability of photocatalytic performance metrics. Throughout this review, percentage-degradation values are quoted because they are the most widely reported figures in the source literature. It must be emphasized, however, that these values are strongly dependent on pollutant identity and concentration, light source spectrum and irradiance, catalyst loading, irradiation time, solution pH, and reactor geometry; direct numerical comparison between studies is therefore unreliable. Where reported, we additionally cite the apparent pseudo-first-order rate constant k (min^{-1}) and, when catalyst mass is given, the mass-normalized rate constant k/m ($\text{L min}^{-1} \text{g}^{-1}$), which provide a more transferable measure of intrinsic photocatalytic activity. We further recommend that future ZnO nanofiber membrane studies adopt standardized benchmark conditions (e.g., 10 mg L^{-1} methylene blue or rhodamine B under defined UV-A irradiance) so that route-level performance can be compared on a common quantitative basis.

Quantitative mechanical and durability comparison. It must first be acknowledged that systematic mechanical characterization (tensile strength, elongation at break, Young's modulus) of ZnO nanofiber membranes is reported only sparsely in the photocatalysis literature; the majority of the studies surveyed here focus on photocatalytic performance and do not include tensile testing. Where data are available, a clear route-dependent trend nonetheless emerges, summarized in Table 5. Pure ceramic ZnO nanofiber membranes are consistently described as brittle, with the calcined product fragmenting on routine handling so that quantitative tensile testing is rarely possible. Hierarchical ZnO/polymer membranes inherit the mechanical compliance of the residual polymer scaffold and remain flexible enough for manual handling, although the secondary ZnO nanostructures may detach under prolonged operation, as reflected in the drop to $\sim 79\%$ retained efficiency after 5 cycles reported by Yan et al. [43]. Composite ZnO/polymer nanofiber membranes exhibit the most robust handling behavior, supporting repeated retrieval and redeployment without macroscopic damage; cycle-stability data are correspondingly more favorable, with Pascariu et al. [67] retaining 97.6% of initial activity over 10 cycles and Jena et al. [70] retaining $>99\%$ over 10 cycles. We emphasize, however, that direct tensile-strength comparison across the routes will only become possible once mechanical testing is adopted as a routine characterization step in this field.

6.2 Performance versus practicality trade-off

Performance–practicality trade-off across the three routes. The cumulative evidence from Tables 1–3, the comparison in Table 4, and the durability summary in Table 5 can be read as a route-by-route trade-off across six practical dimensions: photocatalytic efficiency, specific surface area, mem-

brane flexibility, reusability, scalability, and Zn stability. The *Ceramic Membrane Route* achieves the highest photocatalytic efficiency under UV light (up to 100% degradation of polycyclic aromatic hydrocarbons in $\sim 12 \text{ min}$ [58]) thanks to its high-crystallinity pure ZnO product, but its mechanical brittleness severely limits flexibility, retrievability, and effective reusability, and the bare ZnO surface is the most exposed to photocorrosion. The *Hierarchical Membrane Route* delivers the highest effective surface area through its biomimetic hierarchical morphology and the fastest reported degradation kinetics under simulated sunlight (98.5% MB in 20 min [44]), and the retained polymer scaffold makes the membrane flexible enough to function simultaneously as a microfilter [42]; its main weaknesses are scalability (multi-step batch growth is the principal bottleneck) and a moderate reusability owing to the possibility of secondary-ZnO detachment under prolonged operation, as observed by Yan et al. [43]. The *Composite Membrane Route* is intermediate on photocatalytic efficiency and surface area but excels on the practical axes: it offers the simplest single-step fabrication (best scalability), the most flexible and easily retrievable membranes, the best demonstrated reusability ($>95\%$ retention over 10 cycles [67,70]), and the lowest reported Zn leaching (200-fold reduction versus free powder [64]) thanks to partial polymer encapsulation. No single route therefore dominates on every axis: the Ceramic Route maximizes intrinsic photocatalytic activity, the Hierarchical Route maximizes structural advantages and dual filtration–photocatalysis functionality, and the Composite Route maximizes practical operability and long-term reusability. Selection between them should accordingly be driven by the target application requirements rather than by a single composite score.

We note, however, that these route-level conclusions are subject to substantial inter-study variability. Reported degradation efficiencies span a wide range even within a single route owing to differences in pollutant type and concentration, irradiation source and intensity, catalyst loading, and reactor geometry. Mechanical properties and reusability values are also non-uniformly characterized: certain ceramic membranes reinforced with secondary binders or post-treated with thin polymer overlayers have shown markedly improved handling and retrievability, while a subset of composite membranes have exhibited noticeable performance loss after a few cycles. The route-level rankings presented here therefore reflect the predominant trends in the surveyed literature rather than universal performance hierarchies, and individual systems may deviate considerably from the route-level average.

6.3 Active species and mechanistic insights

Scavenger studies across the three routes reveal interesting mechanistic differences. In the Ceramic Membrane Route, h^+ is consistently identified as the dominant active species [40,41,55], followed by $\cdot\text{O}_2^-$. In the Hierarchical Membrane Route, the dominant species varies with the ZnO modification: $\cdot\text{O}_2^-$ dominates in Sm-doped ZnO/PVDF [42] and ZnO/PPy/PAN [43], while $\cdot\text{OH}$ dominates in the Ag/CuO/ZnO system [44]. This variation likely reflects the different charge transfer pathways enabled by the heterojunction architectures characteristic of the Hierarchical Membrane Route.

Table 4. Comparative analysis of the three electrospinning-based fabrication routes for ZnO nanofiber membrane photocatalysts.

Feature	Ceramic Membrane Route	Hierarchical Membrane Route	Composite Membrane Route
ZnO form	Continuous ceramic NF	Secondary nanostructures on scaffold	Embedded NPs in polymer
ZnO crystallinity	High (calcined at 450–650 °C)	High (grown at 85–140 °C)	Pre-determined by ZnO synthesis
Surface area (m ² /g)	Moderate (12–83)	Enhanced by hierarchy (13–18+)	Low–moderate (17–29)
Membrane flexibility	Brittle (ceramic)	Flexible (polymer retained)	Flexible (polymer retained)
ZnO content	~100% (pure ZnO)	Surface coating	5–40 wt% typical
Processing steps	2 (spin + calcine)	2–3 (spin + seed + grow)	1 (spin only)
Scalability	Moderate	Low (batch growth)	High (single step)
Best reported eff.	100% (PAH, UV) [58]	99% (RhB, sim. sun) [42]	99% (MG, UV) [65]
Best reusability	6 cycles [58]	5 cycles [42]	10 cycles, >99% [70]
Zn leaching	Not reported	Not reported	200× lower [64]
Membrane integration	Difficult (brittle)	Good	Excellent
Water flux	N/A	1620 L m ⁻² h ⁻¹ [42]	Application-dependent
Best suited for	Batch photocatalysis	Hierarchical membrane reactors	Continuous-flow membrane systems

Table 5. Reported durability and handling characteristics of ZnO nanofiber membranes by fabrication route. “NR” = not reported in the source publication. Cycle/retention data are extracted from Tables 1–3; mechanical/handling notes are inferred from descriptions in the source text.

Reference	Route	Cycles	Retention	Tensile	Mechanical / handling note
Singh [58]	Ceramic	6	high	NR	Brittle ceramic mat; handling losses on each cycle
Chen [40]	Ceramic	3	>85%	NR	Brittle on handling
Flores-Garcia [41]	Ceramic	5	64%	NR	Marked degradation after few cycles
Meng [55]	Ceramic	5	NR	NR	Brittle; tested in batch slurry
Pan [42]	Hierarchical	5	stable	NR	Flexible PVDF scaffold; doubles as microfilter
Yan [43]	Hierarchical	5	79%	NR	Drop attributed to ZnO/PPy detachment
Feng [63]	Hierarchical	4	100% ^a	NR	Bactericidal cycles, not dye degradation
Pascariu [67]	Composite	10	97.6% avg	NR	Sacrificial PVP exposes ZnO; flexible
Tissera [64]	Composite	3	~100%	NR	200× lower Zn leaching vs. free powder
Jena [70]	Composite	10	>99%	NR	Mechanically robust; sunlight-active
Parangusan [66]	Composite	NR	NR	NR	Hydrophobic (135 degree); 115% oil uptake

^aBactericidal efficiency, not dye degradation.

7. PHOTOCATALYTIC APPLICATIONS OVERVIEW

7.1 Organic dye degradation

Organic dye degradation remains the most extensively studied application across all three routes [20]. Methylene blue (MB) is the most common model pollutant, followed by Rhodamine B (RhB), Methyl Orange (MO), Malachite Green (MG), and Congo Red (CR). Direct comparison across routes for the same pollutant reveals that Ceramic Membrane Route and Hierarchical Membrane Route products generally achieve faster degradation kinetics under UV light, while Composite Membrane Route products modified with dopants or heterojunctions can achieve competitive performance under visible light or sunlight.

Singh et al. [58] uniquely targeted polycyclic aromatic hydrocarbons (naphthalene and anthracene), which are significantly more challenging substrates than azo or thiazine dyes, demonstrating the capability of high-quality Ceramic Membrane Route nanofibers for treating complex organic pollutants.

7.2 Antibacterial and disinfection applications

A growing number of studies demonstrate the antibacterial capability of electrospun ZnO nanofiber materials, often as a dual function alongside photocatalytic pollutant degradation. The Hierarchical Membrane Route has shown the most impressive disinfection results: Feng et al. [63] achieved 100% killing of both Gram-negative (*E. coli*) and Gram-positive (*S. aureus*) bacteria within 30 min, while Lu et al. [44] reported >99.99% *E. coli* inactivation in 10 min. The Ceramic Membrane Route (Chen et al. [40]: 96–99% bacterial reduction) and the Composite Membrane Route (Herath et al. [68] and Pasindu et al. [69]: inhibition zones 17–33 mm) also demonstrate significant antibacterial activity, though typically at

lower levels.

7.3 Other applications

Parangusan et al. [66] demonstrated a dual photocatalysis–oil absorption function using PVDF/ZnO composite fibers (Composite Membrane Route) with 115% oil uptake capacity and a hydrophobic contact angle of 135 degree. Meng et al. [55] applied Ceramic Membrane Route CuO/ZnO nanofibers for photocatalytic denitrification of simulated fuel oil, representing a novel non-aqueous application. Pan et al. [42] demonstrated that Hierarchical Membrane Route membranes can simultaneously serve as microfilters and photocatalysts, pointing toward integrated water treatment systems. The concept of nanofiber-coated membrane reactors has also been explored for oilfield produced water treatment [71], and electrospun carbohydrate-based nanofiber membranes have shown promise for combined dye and heavy metal removal [72].

8. CHALLENGES AND FUTURE PERSPECTIVES

Prioritization of the outstanding bottlenecks. Before considering route-specific challenges, it is useful to rank the field-wide bottlenecks in order of practical urgency. (1) **Zn leaching and photocorrosion** under prolonged operational conditions remain the single most critical bottleneck for translating ZnO nanofiber membranes from the laboratory to real water-treatment service; this issue is most pressing for ceramic mats and least pressing for well-designed composites where the polymer matrix partially encapsulates the ZnO. (2) **Mechanical and handling robustness** for repeated retrieval and redeployment, particularly under turbulent flow and at scale, is the next most urgent gap and the principal limitation of the Ceramic Route. (3) **Scale-up** from single-needle laboratory electrospinning to needleless or multi-jet configura-

rations capable of producing square-meter membranes with consistent fiber morphology is essential for any commercial pathway, and is currently most severe for the Hierarchical Route owing to its multi-step, batch-bound secondary growth. (4) **Validation in real wastewater matrices**, rather than in single-pollutant model dye solutions, is required to assess fouling resistance, competing-substrate effects, ionic interferences, and long-term stability. The route-specific challenges below should be read against this prioritization.

Despite significant progress, each fabrication route faces distinct challenges that must be addressed for practical implementation:

Ceramic Membrane Route challenges. The mechanical brittleness of calcined ceramic nanofibers remains the most critical limitation. Fiber diameter shrinkage during calcination (typically 50–80% reduction) can cause mat fragmentation. While this route produces the highest-quality ZnO, the inability to form self-standing flexible membranes limits its application to batch reactor configurations. Strategies such as incorporating small amounts of carbon nanofibers or using lower calcination temperatures may partially address this issue.

Hierarchical Membrane Route challenges. The multi-step processing (electrospinning, seeding, and hydrothermal growth, requiring 3–24 h total) limits throughput and scalability. The batch nature of hydrothermal synthesis makes continuous production difficult. Long-term adhesion durability of hydrothermally grown ZnO nanostructures on polymer fibers under continuous operation and mechanical stress needs more investigation, as suggested by the decreased performance observed after 5 cycles in some studies [43].

Composite Membrane Route challenges. ZnO agglomeration at loadings above ~10–15 wt% degrades fiber quality and electrospinnability. The partial embedding of ZnO within the polymer matrix reduces the effective photocatalytic surface area, as quantified by Tissera et al. [64]. Strategies to increase ZnO surface exposure, such as sacrificial pore-forming agents [67], solvent-induced surface enrichment, or post-treatment partial polymer etching, deserve further exploration.

General challenges across all routes:

- **Visible light activation:** Most pure ZnO nanofiber systems are limited to UV activation [17]. While doping and heterojunction strategies have been demonstrated within each route, systematic optimization of visible-light-active compositions across the three fabrication routes remains unexplored.
- **Standardized testing:** The wide variation in experimental conditions (pollutant type and concentration, catalyst loading, light source, and irradiation geometry) makes direct cross-study comparison difficult. Adopting standardized photocatalytic testing protocols would greatly enhance the value of comparative analyses.
- **Long-term stability:** ZnO photocorrosion in aqueous media remains a concern across all routes [45,38], though polymer encapsulation in the Hierarchical and Composite Membrane Routes provides partial protection, as evidenced by the 200-fold reduced zinc leaching reported for the Composite Membrane Route [64].

Scale-up and validation in real wastewater matrices are addressed in the dedicated paragraphs below.

Scale-up: specific research directions. Translation of laboratory ZnO nanofiber membranes to industrial-relevant production hinges on three interlinked questions that have not yet been answered route-by-route. First, the choice of electrospinning configuration: needleless (free-surface), multi-jet, and centrifugal/solution-blowing variants [8,7] differ markedly in their compatibility with high-viscosity polymer/precursor solutions and in the dimensional uniformity they yield, and a comparative evaluation of these configurations specifically for the polymer/precursor systems used in each of the three routes (e.g. ZnAc/PVP, ZnAc/PAN, ZnO-loaded PVDF, PAN/PVDF scaffolds) is currently absent from the literature. Second, the integration of post-electrospinning steps: high-temperature calcination (Ceramic Route) and batch hydrothermal/CBD growth (Hierarchical Route) are the principal scale-up bottlenecks for those routes, and the development of (i) continuous calcination on moving belts under controlled atmosphere, and (ii) flow-through chemical bath deposition or roll-to-roll spray-pyrolysis for secondary growth, would substantially de-risk both routes; the Composite Route, by contrast, requires no post-treatment and its scale-up is principally an electrospinning-throughput problem. Third, fiber-to-fiber and batch-to-batch consistency at scale: characterization protocols quantifying intra-batch fiber-diameter distribution, ZnO loading variance, and photocatalytic-rate-constant variability across square-meter membranes need to be established before any of the routes can credibly claim industrial readiness. We recommend that future scale-up studies report at minimum the throughput (g h^{-1} or $\text{m}^2 \text{h}^{-1}$), the active-area uniformity (coefficient of variation of fiber diameter and ZnO content), and the photocatalytic-activity uniformity across the produced membrane.

Validation in real wastewater matrices: specific research directions. The overwhelming majority of the studies surveyed here employ single-pollutant model dyes (MB, RhB, MO, etc.) in deionized water at neutral pH, conditions that bear little resemblance to actual industrial or municipal wastewater. Several specific gaps therefore deserve targeted investigation. (i) **Co-existing inorganic species:** chloride, bicarbonate, sulfate, phosphate, and dissolved hardness ions (Ca^{2+} , Mg^{2+}) that are abundant in real effluents are known to scavenge reactive oxygen species and can compete with the target pollutant for surface sites; their effect on the apparent rate constant for ZnO nanofiber membranes has not been systematically mapped [2]. (ii) **Natural organic matter (NOM):** humic and fulvic acids attenuate UV/visible light and act as competing photo-sensitizers, and their interaction with ZnO nanofiber membrane surfaces under continuous operation is essentially unstudied. (iii) **Pollutant cocktails:** real wastewater contains mixtures of dyes, pharmaceutical residues, surfactants, and microplastics; the route-specific sensitivity of ZnO nanofiber membranes to such cocktails (and the possible appearance of regio-specific by-products) needs to be assessed. (iv) **Membrane fouling and chemical aging:** adsorption of NOM and biofouling can attenuate photocatalytic activity over time, and a fouling/cleaning protocol analogous to those established for ultrafiltration and microfiltration membranes is required for ZnO photocatalytic membranes. (v) **Pilot-scale validation:** continuous-flow photocatalytic membrane reactors fed with secondary-effluent or surface-water samples [5,6] would provide the strongest evidence of practical viability; such pilots remain rare for ZnO nanofiber membranes specifically. We recommend that future

ZnO nanofiber membrane studies report performance against at least one realistic benchmark matrix (synthetic secondary effluent, real surface water, or industrial dye-house effluent) in addition to standard model-dye experiments.

Future directions. Looking forward, and conditional on overcoming the scalability bottlenecks discussed above, we tentatively identify the **Hierarchical Membrane Route as a particularly promising long-term direction for the field.** Among the three routes, only the Hierarchical Route simultaneously delivers (i) the highest effective surface area through its biomimetic nanorod/nanowire architectures, (ii) the fastest reported degradation kinetics under visible/simulated-sunlight irradiation, and (iii) the unique capacity to combine size-exclusion membrane filtration with in-situ photocatalysis in a single device [42]. These three attributes are precisely what next-generation photocatalytic membrane reactors require, and they cannot be matched by either the Ceramic Route (brittle, non-retrievable) or the Composite Route (partially buried ZnO with intrinsically lower per-mass activity). Realizing this potential, however, requires deliberate engineering effort along several fronts:

- *Continuous and lower-temperature secondary growth.* Replacing batch hydrothermal autoclaves with flow-through chemical bath deposition or low-temperature solution growth could turn the rate-limiting step of the Hierarchical Route into a continuous operation compatible with roll-to-roll electrospinning lines.
- *Robust ZnO/polymer interfacial adhesion.* The decreased reuse efficiency observed after several cycles in some Hierarchical Route systems [43] points to nanostructure detachment. Surface functionalization of the polymer scaffold and gradient interlayers (e.g., seeded ZnO underlayers) could anchor the secondary nanostructures more durably.
- *Integrated photocatalytic membrane reactor design.* The dual filtration–degradation functionality demonstrated by Pan et al. [42], with a water flux of 1620 Lpermsquaredperh, should be evaluated under realistic crossflow operation, multi-pollutant feeds, and prolonged duty cycles to establish whether hierarchical ZnO membranes can replace multi-stage treatment trains.
- *Hybrid routes leveraging the strengths of multiple strategies.* For instance, calcined Ceramic Route fibers can serve as templates for subsequent Hierarchical Route secondary growth, combining the high crystallinity of the former with the surface area and dual-functionality of the latter.

In parallel, several broader research priorities apply across all three routes: (i) machine learning optimization of electrospinning and growth parameters; (ii) scale-up to continuous, needleless or multi-jet electrospinning with in-line post-treatment; (iii) systematic exploration of visible-light-active compositions through doping and heterojunction engineering [17]; (iv) coupling with complementary treatment processes such as adsorption–photocatalysis and photocatalytic membrane reactor configurations [5,6,2]; and (v) emerging synergistic mechanisms such as piezo-photocatalysis [61], which exploits the inherent piezoelectric properties of ZnO nanostructures to generate additional charge carriers under mechanical stress.

9. CONCLUSION

This review has classified and compared three electrospinning-based fabrication routes for ZnO nanofiber membrane photocatalysts. The choice of route fundamentally determines product characteristics, photocatalytic behavior, and, crucially, the ease of membrane retrieval and reuse.

The Ceramic Membrane Route produces pure ceramic ZnO nanofiber membranes with high crystallinity and up to 100% degradation efficiency under UV light. However, the brittle nature of the calcined product severely compromises membrane retrieval, as the ceramic mat fragments upon handling. This route is best suited for high-performance batch photocatalytic applications where the membrane remains stationary.

The Composite Membrane Route offers the simplest single-step fabrication, the best demonstrated reusability (up to 10 cycles with 97–99% efficiency retention), the lowest zinc leaching (200-fold reduction versus free powder), and the most straightforward membrane retrieval. The flexible membrane can be lifted from treated water, rinsed, and redeployed without structural degradation. Although photocatalytic efficiency per unit ZnO is lower due to partial polymer embedding, the practical advantages of easy retrieval and sustained performance position the Composite Membrane Route as one of the more operationally mature options for near-term, real-world deployment.

The Hierarchical Membrane Route creates hierarchical structures with the largest effective surface area and the fastest degradation kinetics (98.5% MB in 20 min). It uniquely combines photocatalytic and membrane filtration functionality in a single device while retaining the mechanical flexibility of the polymer backbone for intact membrane retrieval. Although the current multi-step, batch-dependent processing limits scalability, these intrinsic performance advantages identify the Hierarchical Membrane Route as a particularly promising long-term direction for the field, conditional on those scalability bottlenecks being addressed. Targeted development of continuous, lower-temperature, and seedless growth strategies could unlock scalable hierarchical membrane reactors that combine pollutant filtration and degradation in a single integrated step, an outcome that neither the Ceramic nor the Composite Route can match by design.

The choice of fabrication route should therefore be guided by both the target application and the developmental horizon. For near-term deployment in continuous-flow water treatment systems, the Composite Membrane Route is currently the most realistic option, owing to its single-step fabrication, demonstrated long-cycle reusability, and minimal zinc leaching. For high-performance batch reactors where membrane mobility is not required, the Ceramic Membrane Route remains attractive. Looking ahead, however, the Hierarchical Membrane Route emerges as a particularly promising long-term direction. Future research should prioritize continuous and scalable secondary-growth strategies, robust ZnO-to-polymer adhesion under prolonged operation, and integrated photocatalytic membrane reactor designs that fully exploit its dual filtration–degradation capability. Across all three routes, standardized testing protocols, evaluation in real wastewater matrices, and long-term membrane retrieval durability studies will be essential to translate laboratory demonstrations into deployed water treatment technologies.

ACKNOWLEDGMENTS

This study received no funding.

CONFLICT OF INTEREST

The authors declare that they have no known competing financial interests or personal relationships that could have appeared to influence the work reported in this paper.

REFERENCES

- [1] Byrne Ciara, Subramanian Gokulakrishnan, Pillai Suresh C.. Recent advances in photocatalysis for environmental applications. *Journal of Environmental Chemical Engineering*. 2018;6:3531-3555. doi:10.1016/j.jece.2017.07.080.
- [2] Koe Wei Song, Lee Jia Wei, Chong Woon Chan, Pang Yean Ling, Sim Lan Ching. An overview of photocatalytic degradation: photocatalysts, mechanisms, and development of photocatalytic membrane. *Environmental Science and Pollution Research*. 2020;27:2522-2565. doi:10.1007/s11356-019-07193-5.
- [3] Lee Kian Mun, Lai Chin Wei, Ngai Koh Sing, Juan Joon Ching. Recent developments of zinc oxide based photocatalyst in water treatment technology: A review. *Water Research*. 2016;88:428-448. doi:10.1016/j.watres.2015.09.045.
- [4] Ong Chi Boon, Ng Law Yong, Mohammad Abdul Wahab. A review of ZnO nanoparticles as solar photocatalysts: Synthesis, mechanisms and applications. *Renewable and Sustainable Energy Reviews*. 2018;81:536-551. doi:10.1016/j.rser.2017.08.020.
- [5] Mozia Sylwia. Photocatalytic membrane reactors (PMRs) in water and wastewater treatment. A review. *Separation and Purification Technology*. 2010;73:71-91. doi:10.1016/j.seppur.2010.03.021.
- [6] Leong Siewhui, Razmjou Amir, Wang Kun, Hapgood Karen, Zhang Xiwang, Wang Huanting. TiO₂ based photocatalytic membranes: A review. *Journal of Membrane Science*. 2014;472:167-184. doi:10.1016/j.memsci.2014.08.016.
- [7] Xue Jiajia, Wu Tong, Dai Yunqian, Xia Younan. Electrospinning and electrospun nanofibers: Methods, materials, and applications. *Chemical Reviews*. 2019;119:5298-5415. doi:10.1021/acs.chemrev.8b00593.
- [8] Persano Luana, Camposeo Andrea, Tekmen Cagri, Pisignano Dario. Industrial upscaling of electrospinning and applications of polymer nanofibers: A review. *Macromolecular Materials and Engineering*. 2013;298:504-520. doi:10.1002/mame.201200290.
- [9] Nasir Atikah Mohd, Awang Nuha, Jaafar Juhana, Ismail Ahmad Fauzi, Othman Mohd Hafiz Dzarfan, Rahman Mukhlis A., Aziz Farhana, Yajid Muhamad Azizi Mat. Recent progress on fabrication and application of electrospun nanofibrous photocatalytic membranes for wastewater treatment: A review. *Journal of Water Process Engineering*. 2021;40:101878. doi:10.1016/j.jwpe.2020.101878.
- [10] Cordoba Alexander, Saldias Cesar, Urzúa Marcela, Montalti Marco, Guernelli Moreno, Focarete Maria Letizia, Leiva Angel. On the versatile role of electrospun polymer nanofibers as photocatalytic hybrid materials applied to contaminated water remediation: A brief review. *Nanomaterials*. 2022;12:756. doi:10.3390/nano12050756.
- [11] Mapukata Sivuyisiwe, Shingange Katekani, Mokhena Teboho. Review of the recent advances on the fabrication, modification and application of electrospun TiO₂ and ZnO nanofibers for the treatment of organic pollutants in wastewater. *Frontiers in Chemical Engineering*. 2023;5:1304128. doi:10.3389/fceng.2023.1304128.
- [12] Serik Aigerim, Idrissov Nurlan, Baratov Aibol, Dikov Alexey, Kislitsin Sergey, Daulbayev Chingis, Kusanov Zhengisbek. Recent progress in photocatalytic applications of electrospun nanofibers: A review. *Molecules*. 2024;29:4824. doi:10.3390/molecules29204824.
- [13] Mhalshekar Krushika, Krishan Anurag, Gaydhane Mrunalini, Sontakke Sharad, Pawar Vivek. Advanced electrospun nanofibers for photocatalytic degradation: Sustainable solutions for wastewater remediation. *ACS Omega*. 2026;11:6954-6985. doi:10.1021/acsomega.5c10970.
- [14] Sarkodie Benjamin, Amesimeku Joshua, Frimpong Charles, Howard Ebenezer Kofi, Feng Quan, Xu Zhenzhen. Photocatalytic degradation of dyes by novel electrospun nanofibers: A review. *Chemosphere*. 2023;313:137654. doi:10.1016/j.chemosphere.2022.137654.
- [15] Panda Pravat Kumar, Sahoo Biswajit, Ramakrishna Seeram. Electrospun nanofibers for photocatalytic water treatment and hydrogen generation application: A review. *International Journal of Hydrogen Energy*. 2023;48:37193-37208. doi:10.1016/j.ijhydene.2023.06.151.
- [16] Lu Na, Zhang Mingming, Jing Xueru, Zhang Pengfei, Zhu Yongan, Zhang Zhenyi. Electrospun semiconductor-based nano-heterostructures for photocatalytic energy conversion and environmental remediation: Opportunities and challenges. *Energy and Environmental Materials*. 2023;6:e12338. doi:10.1002/eem2.12338.
- [17] Samadi Morasae, Zirak Mahdi, Naseri Amene, Khorashadizade Elham, Moshfegh Alireza Z.. Recent progress on doped ZnO nanostructures for visible-light photocatalysis. *Thin Solid Films*. 2016;605:2-19. doi:10.1016/j.tsf.2015.12.064.
- [18] Rianjanu Aditya, Nurfitri Rima, Nurfani Eka, Aflaha Rizky, Triyana Kuwat, Taher Tarmizi, Andreani Agustina Sus, Gultom Noto Susanto, Widakdo Januar, Hapidin Dian Ahmad, Peiner Erwin, Wasisto Hutomo Suryo. Unlocking the full potential of zinc oxide/cerium oxide composite nanoparticles for removal of mixed pharmaceutical and dye pollutants in water. *Advanced Materials Interfaces*. 2026;70472. doi:10.1002/admi.70472.
- [19] Pascariu Petronela, Homocianu Mihaela. ZnO-based ceramic nanofibers: Preparation, properties and applications. *Ceramics International*. 2022;48:18467-18501. doi:10.1016/j.ceramint.2022.03.128.
- [20] Rianjanu Aditya. Recent advances in electrospun nanofiber membranes for dye filtration: A focused mini-review. *Environmental Chemistry and Safety*. 2025;1:9600018. doi:10.26599/ECS.2025.9600018.
- [21] Baig Aliya, Siddique Mohsin, Panchal Suman. A review of visible-light-active zinc oxide photocatalysts for environmental application. *Catalysts*. 2025;15:100. doi:10.3390/catal15020100.
- [22] Sanakousar F. M., Vidyasagar C. C., Jimenez-Perez V. M., Prakash K.. Recent progress on visible-light-driven metal and non-metal doped ZnO nanostructures for photocatalytic degradation of organic pollutants. *Materials Science in Semiconductor Processing*. 2022;140:106390. doi:10.1016/j.mssp.2021.106390.
- [23] Zheng Andrew Lim Teik, Abdullah Che Azurahaman Che, Chung Eric Lim Teik, Andou Yoshito. Recent progress in visible light-doped ZnO photocatalyst for pollution control. *International Journal of Environmental Science and Technology*. 2023;20:5753-5772. doi:10.1007/s13762-022-04354-x.
- [24] Mao Tianhao, Liu Mingyue, Lin Lina, Cheng Yuting, Fang Chunhua. A study on doping and compound of zinc oxide photocatalysts. *Polymers*. 2022;14:4484. doi:10.3390/polym14214484.
- [25] Ahmad Iqbal, Bousbih Rim, Mahal Ahmed, Henaish Ahmed, Alharthi Sarah, Alharthi Najla S., Aldhafeeri Nawaf, Alanazi Maha M., Almisri Abdulaziz N., Alhomaidei Eman A., Alanazi Yasmeen M., Alanazi Mohammed M., Alanazi Abdullah M.. Recent progress in ZnO-based heterostructured photocatalysts: A review. *Materials Science in Semiconductor Processing*. 2024;180:108578. doi:10.1016/j.mssp.2024.108578.
- [26] Dhiman Pankaj, Rana Garima, Kumar Amit, Sharma Gaurav, Vo Dai-Viet N., Naushad Mu.. ZnO-based heterostructures as photocatalysts for hydrogen generation and depollution: A review. *Environmental Chemistry Letters*. 2022;20:1047-1081. doi:10.1007/s10311-021-01361-1.
- [27] Rasheed Hafiz Muhammad, Aroosh Komal, Meng Daimei, Ruan Xianguang, Akhter Mohsina, Cui Xiaoqiang. A review on modified ZnO to address environmental challenges through photocatalysis: Photodegradation of organic pollutants. *Materials Today Energy*. 2025;48:101774. doi:10.1016/j.mtener.2024.101774.

- [28] Abdul Halim Othman M., Mustapha Nurul Hidayah, Mohd Fudzi Siti Nor, Azhar Roshazma, Zanal Nor Izzah Najwa, Nazua Nur Farhana, Nordin Ahmad Hafiz, Mohd Azami Mohd Sufri, Mohd Ishak Mohd Azlan, Wan Ismail Wan Iryani Najwa, Ahmad Zulkifli. A review on modified ZnO for the effective degradation of methylene blue and rhodamine B. *Results in Surfaces and Interfaces*. 2025;18:100408. doi:10.1016/j.rsufi.2024.100408.
- [29] Abdullah Fatin Hanani, Abu Bakar Noor Haida Hayati, Abu Bakar Mohamad. Current advancements on the fabrication, modification, and industrial application of zinc oxide as photocatalyst in the removal of organic and inorganic contaminants in aquatic systems. *Journal of Hazardous Materials*. 2022;424:127416. doi:10.1016/j.jhazmat.2021.127416.
- [30] Abou Zeid Sara, Leprince-Wang Yamin. Advancements in ZnO-based photocatalysts for water treatment: A comprehensive review. *Crystals*. 2024;14:611. doi:10.3390/cryst14070611.
- [31] Zhu Chuang, Wang Xin. Nanomaterial ZnO synthesis and its photocatalytic applications: A review. *Nanomaterials*. 2025;15:682. doi:10.3390/nano15090682.
- [32] Kadhim Mustafa Jasim, Mahdi Mohammed A., Selman Ahmed M., Al-Ani Sabah K. J., Hassan Jamal J., Ahmed Naser M.. The most important parameters that affect the photocatalytic activity of ZnO nanostructures against organic dyes: A review. *Iranian Journal of Catalysis*. 2023;13:1-21. doi:10.30495/ijc.2023.1969439.1966.
- [33] Ghamarpoor Reza, Fallah Atefeh, Jamshidi Masoud. A review of synthesis methods, modifications, and mechanisms of ZnO/TiO₂-based photocatalysts for photodegradation of contaminants. *ACS Omega*. 2024;9:25457-25492. doi:10.1021/acsomega.3c08717.
- [34] AlMohamadi Hamad, Awad Sherif A., Sharma Anjan Kumar, Fayzullaev Normurot, T'avaara-Aponte Alfonso, Chiguala-Contreras Liz, Amari Abdelfattah, Rodriguez-Benites Carmen, Tahoon Mohamed A., Esmaili Hossein. Photocatalytic activity of metal- and non-metal-anchored ZnO and TiO₂-based photocatalysts for advanced photocatalysis: Comparative study. *Catalysts*. 2024;14:420. doi:10.3390/catal14070420.
- [35] Abdul Mutalib Aishah Aqilah, Jaafar Nur Farhana. ZnO photocatalysts applications in abating the organic pollutant contamination: A mini review. *Total Environment Research Themes*. 2022;1-2:100013. doi:10.1016/j.totert.2022.100013.
- [36] G'uell Frank, Gald'amez-Mart'inez Andr'es, Mart'inez-Alanis Paulina R., Catto Ariadne C., da Silva Luis F., Mastelaro Valmor R., Santana Guillermo, Dutt Ateet. ZnO-based nanomaterials approach for photocatalytic and sensing applications: Recent progress and trends. *Materials Advances*. 2023;4:3685-3707. doi:10.1039/D3MA00227F.
- [37] Kazemi Hakki Hossein, Sillanp'a' Mika. Comprehensive analysis of photocatalytic and photoreactor challenges in photocatalytic wastewater treatment: A case study with ZnO photocatalyst. *Materials Science in Semiconductor Processing*. 2024;181:108592. doi:10.1016/j.mssp.2024.108592.
- [38] Kisslinger Ryan, Hua Weizhi, Shankar Karthik. Bulk and surface properties of zinc oxide. *Physical Chemistry Chemical Physics*. 2017;19:20104-20123. doi:10.1039/C7CP03434A.
- [39] Zhang Qifeng, Dandeneau Christopher S., Zhou Xiaoyuan, Cao Guozhong. ZnO nanostructures for dye-sensitized solar cells. *Advanced Materials*. 2009;21:4087-4108. doi:10.1002/adma.200803827.
- [40] Chen Ru, Tian Si-meng, Song Jing-hui, Zhao Guang-tai, Cao Xin-miao, Shi Qing-yu, Gong Weitao. Preparation of zinc oxide nanofibers and their photocatalytic degradation and antibacterial properties. *Colloid and Polymer Science*. 2025;303:2167-2177. doi:10.1007/s00396-025-05472-x.
- [41] Flores-Garcia E., Hernandez-Landaverde M. A., Romero-Avila E., Ramirez-Bon R.. ZnO crystalline nanofibers with photocatalytic properties obtained from pork skin gelatin and zinc acetate fibers. *Journal of Materials Science: Materials in Electronics*. 2025;36:1662. doi:10.1007/s10854-025-15703-0.
- [42] Pan Tiandi, Liu Yong, Li Zongjie, Fan Jie, Wang Liang, Liu Jian, Shou Wan. A Sm-doped Egeria-densa-like ZnO nanowires@PVDF nanofiber membrane for high-efficiency water clean. *Science of the Total Environment*. 2020;737:139818. doi:10.1016/j.scitotenv.2020.139818.
- [43] Yan Hongsheng, Xiong Jie, Du Peijian, Wu Ermiao, Pan Tiandi, Li Ni. Construction of ZnO/PPy/PAN nanofiber membrane as heterojunction photocatalyst with enhanced photocatalytic activity. *Fibers and Polymers*. 2025;26:589-596. doi:10.1007/s12221-024-00839-3.
- [44] Lu Wei, Gu Tongtong, Jing Xuedong, Zhu Yongan, Yu Linqun, Hou Shichao, Pang Tingting, Lu Na, Zhang Zhenyi. Ag nanoparticles-decorated p-type CuO/n-type ZnO heterojunction nanofibers with enhanced photocatalytic activities for dye degradation and disinfection. *Journal of Alloys and Compounds*. 2023;968:171864. doi:10.1016/j.jallcom.2023.171864.
- [45] Han Jingbo, Qiu Wei, Gao Wei. Potential dissolution and photo-dissolution of ZnO thin films. *Journal of Hazardous Materials*. 2010;178:115-122. doi:10.1016/j.jhazmat.2010.01.050.
- [46] Aflaha Rizky, Putri Linda Ardita, Farrel Aloysius, Anzinger Sebastian, Rianjanu Aditya, Yulianto Nursidik, Fueldner Marc, Roto Roto, Peiner Erwin, Wasisto Hutomo Suryo, Triyana Kuwat. Crafting high-temperature stable and hydrophobic nanofiber membranes for particulate matter filtration. *Communications Materials*. 2025;6:107. doi:10.1038/s43246-025-00799-y.
- [47] Rianjanu Aditya, Roto Roto, Julian Trisna, Hidayat Shidiq Nur, Kusumaatmaja Ahmad, Suyono Eko Agus, Triyana Kuwat. Polyacrylonitrile nanofiber-based quartz crystal microbalance for sensitive detection of safrole. *Sensors*. 2018;18:1150. doi:10.3390/s18041150.
- [48] Chotimah, Rianjanu Aditya, Winardianto Bimo, Munir Misbachul, Kartini Indriana, Triyana Kuwat. Electrical conductivity improvement of polyvinyl alcohol nanofiber by solvent vapour treatment. *International Journal on Advanced Science, Engineering and Information Technology*. 2016;6:675-681. doi:10.18517/ijaseit.6.5.1055.
- [49] Aflaha Rizky, Putri Linda Ardita, Maharani Chlara Naren, Rianjanu Aditya, Roto Roto, Wasisto Hutomo Suryo, Triyana Kuwat. Tuning a superhydrophobic surface on an electrospun polyacrylonitrile nanofiber membrane by polysulfone blending. *ACS Omega*. 2024;9:29840-29847. doi:10.1021/acsomega.4c03554.
- [50] Rianjanu Aditya, Kusumaatmaja Ahmad, Suyono Eko Agus, Triyana Kuwat. Solvent vapor treatment improves mechanical strength of electrospun polyvinyl alcohol nanofibers. *Heliyon*. 2018;4:e00592. doi:10.1016/j.heliyon.2018.e00592.
- [51] Aflaha Rizky, Maharani Chlara Naren, Putri Linda Ardita, Prabowo Yuliyani Dwi, Rahman Iman, Taher Tarmizi, Rianjanu Aditya, Roto Roto, Wasisto Hutomo Suryo, Triyana Kuwat. A superhydrophobic and heat-resistant PAN/PSU/PTFE composite nanofiber membrane for high-efficiency PM. *Materials Advances*. 2024;5:9215-9226. doi:10.1039/d4ma00841c.
- [52] Cao Yilin, Xu Lan. Hollow ZnO nanofibers for efficient photocatalytic degradation of methylene blue. *Catalysts*. 2025;15:1137. doi:10.3390/catal15121137.
- [53] Yang Yaoyao, Zhou Shengwei, Cao Xianyang, Lv He, Liang Zhiyuan, Zhang Rui, Ye Fujia, Yu Dengguang. Coaxial electrospun porous core-shell nanofibrous membranes for photodegradation of organic dyes. *Polymers*. 2024;16:754. doi:10.3390/polym16060754.
- [54] Kim Wan-Tae, Na Kyeong-Han, Park Dong-Cheol, Yang Wan-Hee, Choi Won-Youl. Photocatalytic methylene blue degradation of electrospun Ti-Zn complex oxide nanofibers. *Nanomaterials*. 2020;10:1311. doi:10.3390/nano10071311.
- [55] Meng Qingming, Liu Wenna, Jiang Juan, Zhang Xinle. Fabrication of novel p-CuO/n-ZnO heterojunction nanofibers by electrospinning for enhanced photocatalytic performance in the denitrification of fuel oil. *Ceramics International*. 2021;47:19402-19413. doi:10.1016/j.ceramint.2021.03.277.
- [56] Liu Liu, Liu Zhiwei, Yang Yixin, Geng Mingqian, Zou Yiming, Shahzad M. Babar, Dai Yuxiang, Qi Yang. Photocatalytic properties of Fe-doped ZnO electrospun nanofibers. *Ceramics International*. 2018;44:19998-20005. doi:10.1016/j.ceramint.2018.07.267.

- [57] Naseri Amene, Samadi Morasae, Pourjavadi Ali, Ramakrishna Seeram, Moshfegh Alireza Z.. Enhanced photocatalytic activity of ZnO/g-C₃N₄ nanofibers constituting carbonaceous species under simulated sunlight for organic dye removal. *Ceramics International*. 2021;47:26185-26196. doi:10.1016/j.ceramint.2021.06.025.
- [58] Singh Puneet, Mondal Kunal, Sharma Ashutosh. Reusable electrospun mesoporous ZnO nanofiber mats for photocatalytic degradation of polycyclic aromatic hydrocarbon dyes in wastewater. *Journal of Colloid and Interface Science*. 2013;394:208-215. doi:10.1016/j.jcis.2012.12.006.
- [59] Pantò Fabiola, Dahrouch Zainab, Saha Abhirup, Patan\`e Salvatore, Santangelo Saveria, Triolo Claudia. Photocatalytic degradation of methylene blue dye by porous zinc oxide nanofibers prepared via electrospinning: When defects become merits. *Applied Surface Science*. 2021;557:149830. doi:10.1016/j.apsusc.2021.149830.
- [60] Chen Mingyi, Liu Peng, He Ji-Huan, Wang Hsing-Lin, Zhang Haonan, Wang Xin, Chen Rouxi. Nanofiber template-induced preparation of ZnO nanocrystal and its application in photocatalysis. *Scientific Reports*. 2021;11:21196. doi:10.1038/s41598-021-00303-9.
- [61] Asghari Sarabi Ghazale, Samadi Morasae, Bagheri Habib, Kibria Md. Golam, Moshfegh Alireza Z.. Floating Ag-ZnO@PAN nanofiber mats with photocatalytic, piezoelectric, and plasmonic functions for wastewater treatment. *Research on Chemical Intermediates*. 2025;51:6487-6514. doi:10.1007/s11164-025-05759-2.
- [62] Araújo Evando S., da Costa Bruna P., Oliveira Raquel A. P., Libardi Juliano, Faia Pedro M., de Oliveira Helinando P. TiO₂/ZnO hierarchical heteronanostructures: Synthesis, characterization and application as photocatalysts. *Journal of Environmental Chemical Engineering*. 2016;4:2820-2829. doi:10.1016/j.jece.2016.05.021.
- [63] Feng Lian, Zhang Penghao, Li Yuan, Ye Fangxin, Ma Yanze, He Gongtian, Lv Mingyu, Zhang Tian. Controllable fabrication of Ag/ZnO/g-C₃N₄ nanofiber heterojunctions for enhanced photocatalytic water disinfection. *Frontiers of Materials Science*. 2025;19:250720. doi:10.1007/s11706-025-0720-5.
- [64] Tissera Nadeeka D., Wijesena Ruchira N., Sandaruwan Chanaka S., de Silva Rohini M., de Alwis Ajith, de Silva K. M. Nalin. Photocatalytic activity of ZnO nanoparticle encapsulated poly(acrylonitrile) nanofibers. *Materials Chemistry and Physics*. 2018;204:195-206. doi:10.1016/j.matchemphys.2017.10.035.
- [65] Yar Adem, Haspulat Bircan, Ustun Tugay, Eskizeybek Volkan, Avci Ahmet, Kamis Handan, Achour Slimane. Electrospun TiO₂/ZnO/PAN hybrid nanofiber membranes with efficient photocatalytic activity. *RSC Advances*. 2017;7:29806-29814. doi:10.1039/c7ra03699j.
- [66] Parangusan Hemalatha, Bhadra Jolly, Ahmad Zubair, Al-Maadeed Ali S. M. A., Al-Mohannadi Abdulaziz M. A. A., Al-Thani Noora. Electrospun PVDF/ZnO based composite fibers for oil absorption and photocatalytic degradation of organic dyes from waste water. *Fibers and Polymers*. 2022;23:1217-1224. doi:10.1007/s12221-022-4542-0.
- [67] Pascariu Petronela, Cojocaru Corneliu, Samoila Petrisor, Olaru Niculae, Bele Adrian, Airinei Anton. Novel electrospun membranes based on PVDF fibers embedding lanthanide doped ZnO for adsorption and photocatalytic degradation of dye organic pollutants. *Materials Research Bulletin*. 2021;141:111376. doi:10.1016/j.materresbull.2021.111376.
- [68] Herath Hasitha, Pasindu Viduranga, Yapa Piumika, Dabare Sanduni, Munaweera Imalka, Weerasekera Manjula M., Samarakoon Upeka. Fabrication and characterization of Cu-ZnO-cellulose acetate electrospun nanocomposite membranes for dual-function photocatalytic degradation and microbial inhibition. *Materials Advances*. 2025;6:8092-8113. doi:10.1039/d5ma00890e.
- [69] Pasindu Viraj, Yapa Piumika, Dabare Sanduni, Munaweera Imalka, Etampawala Thusitha, Weerasekera Manjula M., Attygalle Dinesh, Amarasinghe Shantha. Harnessing the power of visible light with GO-Ni-ZnO nanohybrid electrospun polymeric membranes for improved photocatalysis: a focused approach to fabrication, characterization, and applications. *Emergent Materials*. 2025;8:6817-6842. doi:10.1007/s42247-025-01188-4.
- [70] Jena Sandeep Kumar, Sadasivam Rajkumar, Packirisamy Gopinath, Saravanan Pichiah. Nanoremediation: Sunlight mediated dye degradation using electrospun PAN/CuO-ZnO nanofibrous composites. *Environmental Pollution*. 2021;280:116964. doi:10.1016/j.envpol.2021.116964.
- [71] Alias Nur Hanis, Jaafar Juhana, Samitsu Sadaki, Matsuura Takeshi, Ismail Ahmad Fauzi, Othman Mohd Hafiz Dzarfan, Rahman Mukhlis A., Othman Nor Haniza, Paiman Norhaniza, Yusof Norhaniza, Aziz Farhana. Photocatalytic nanofiber-coated alumina hollow fiber membranes for highly efficient oilfield produced water treatment. *Chemical Engineering Journal*. 2019;360:1437-1446. doi:10.1016/j.cej.2018.10.217.
- [72] Phan Duy-Nam, Khan Muhammad Qamar, Nguyen Nien-Tzu, Phan Thanh-Truc, Ullah Amin, Khatri Muzamil, Kien Nguyen Ngoc, Kim Ick-Soo. A review on the fabrication of several carbohydrate polymers into nanofibrous structures using electrospinning for removal of metal ions and dyes. *Carbohydrate Polymers*. 2021;252:117175. doi:10.1016/j.carbpol.2020.117175.